Published in final edited form as:

FASEB J. 2021 September ; 35(9): e21797. doi:10.1096/fj.202100495R.

Ablation of PDE4B protects from *Pseudomonas aeruginosa*-induced acute lung injury in mice by ameliorating the cytostorm and associated hypothermia

Lina Abou Saleh[1,4], **Abigail Boyd**[1,4], **Ileana V. Aragon**[1,4], **Anna Koloteva**[1,4], **Domenico Spadafora**[2], **Wadad Mneimneh**[3], **Robert A. Barrington**[2], **Wito Richter**[1,4]

[1]Department of Biochemistry & Molecular Biology, University of South Alabama, College of Medicine, Mobile, AL.

[2]Department of Microbiology & Immunology, University of South Alabama, College of Medicine, Mobile, AL.

[3]Department of Pathology, University of South Alabama, College of Medicine, Mobile, AL.

[4]Center for Lung Biology, University of South Alabama, College of Medicine, Mobile, AL.

Abstract

Pseudomonas aeruginosa is a frequent cause of hospital-acquired lung infections characterized by hyperinflammation, antibiotic resistance, and high morbidity/mortality. Here, we show that genetic ablation of one cAMP-phosphodiesterase 4 subtype, PDE4B, is sufficient to protect mice from acute lung injury induced by *P. aeruginosa* infection, as it reduces pulmonary and systemic levels of pro-inflammatory cytokines, as well as pulmonary vascular leakage and mortality. Surprisingly, despite dampening immune responses, bacterial clearance in lungs of PDE4B-KO mice is significantly improved compared to WT controls. In wildtypes, *P. aeruginosa* infection produces high systemic levels of several cytokines, including TNF-α, IL-1β, and IL-6, that act as cryogens and render the animals hypothermic. This, in turn, diminishes their ability to clear the bacteria. Ablation of PDE4B curbs both the initial production of acute-response cytokines, including TNF-α and IL-1β, as well as their downstream signaling, specifically the induction of the secondary-response cytokine IL-6. This synergistic action protects PDE4B-KO mice from the deleterious effects of the *P. aeruginosa*-induced cytostorm, while concurrently improving bacterial clearance, rather than being immunosuppressive. These effects of PDE4B ablation are contrary to those resulting from treatment with PAN-PDE4 inhibitors, which have been shown to increase bacterial burden and dissemination. Thus, PDE4B represents a promising therapeutic target in settings of *P. aeruginosa* lung infections.

Correspondence: Wito Richter, Department of Biochemistry & Molecular Biology, Center for Lung Biology, University of South Alabama College of Medicine, 5851 USA Drive North, MSB2310, Mobile, AL 36688, USA, richter@southalabama.edu, Phone: 251-414-8298, FAX: 251-460-6850.

Author contributions:

LA, RAB, and WR designed the experiments; LA, IVA, AB, and WR performed animal experimentation and measurement of cytokines and cell- and bacterial counts; LA, DS, and RAB performed flow cytometry and analysis; WM scored lung tissue sections; IVA, AB, AK and WR generated the animals and maintained the colonies; LA performed the cell culture and siRNA experiments; all authors contributed to data analyses; LA and WR wrote a draft and all authors edited and approved the manuscript.

Declaration of conflicts of interest: none

Keywords

PDE4B; cytostorm; hypothermia; *Pseudomonas aeruginosa* ; acute lung injury; interleukin 6

1. INTRODUCTION

Pseudomonas aeruginosa (*PA*) is a leading cause of hospital-acquired lung infections such as ventilator-associated pneumonia (VAP)[1, 2]. Particularly in critically ill or immunocompromised patients, pulmonary *PA* infections often progress to cause severe lung injury that is characterized by hyperinflammation and alveolar/vascular barrier dysfunction, leading to edema, alveolar flooding, and eventually respiratory distress. In addition, *PA* lung infections are associated with systemic inflammation and injury including sepsis and multi-organ dysfunction, such as acute kidney injury or neurologic dysfunctions. Further complicating treatment, *PA* exhibits high rates of antibiotic resistance, for which reason the World Health Organization ranked this bacterium 2nd on its list of "Priority Pathogens" in 2017. Despite significant research efforts, there are few effective treatments and morbidity and mortality (~30%) in *PA* pneumonia patients remain high, underlining an urgent need for novel treatment strategies[3].

It is well established that inhibitors of Type 4 cyclic nucleotide phosphodiesterases (PDE4s), a group of isoenzymes that hydrolyze and inactivate the second messenger cAMP, exert broad-spectrum anti-inflammatory properties in humans and animals alike. PDE4 inhibitors are currently being developed and/or clinically used as anti-inflammatory therapies for a variety of conditions ranging from psoriasis to arthritis, inflammatory bowel disease, or neuroinflammation[4]. PDE4 inhibitors have also shown efficacy in preclinical models of acute lung injury, such as after instillation of *E.coli* lipopolysaccharide (LPS) in mice, and are pursued as treatments for other inflammatory lung diseases, including asthma and COPD[5, 6]. However, the clinical success of PDE4 inhibitors has been somewhat muted due to a narrow therapeutic window, defined by nausea and emesis as the most common side effects, that is characteristic for this class of drugs[5, 7]. The PDE4 family comprises four genes, PDE4A to PDE4D, and each is expressed as multiple protein variants[8]. Genetic ablation of each of the four PDE4 subtypes in mice, or their siRNA-mediated knockdown in cells, produces distinct phenotypes, suggesting that individual PDE4s serve unique and non-overlapping molecular, cellular and physiological functions. Thus, targeting individual PDE4 subtypes is a promising approach to separate the therapeutically beneficial from the side effects of the non-selective PDE4 inhibitors available to date[5, 7, 9]. Ablation of PDE4B, specifically the PDE4B splicing variant PDE4B2, impairs production of several inflammatory cytokines including TNF-α (in LPS models) or TH_2-cytokines (in asthma models) [10–13], and may thereby reduce pulmonary and/or systemic injury. Thus, PDE4B2 is thought to be a primary target by which PAN-PDE4 inhibitors reduce inflammation. Here, we tested whether the anti-inflammatory benefits reported in non-infectious and/or sterile models of lung inflammation are retained in a model of severe acute lung injury induced by infection with a live bacterial pathogen. Given the persistent antibiotic resistance of *PA,* we specifically aimed to determine whether dampening the body's immune responses *via* PDE4B inactivation would affect bacterial load and/or survival in the absence of antibiotic

treatment. We find that in wildtype cells or animals, PDE4B expression is upregulated in response to the detection of the bacterial pathogen (e.g. LPS/TLR4) and, independently, in response to the presence of acute-response cytokines, such as TNF-α and IL-1β. PDE4B induction, in turn, removes the negative constraint of cellular cAMP signaling on the hyper-production of pro-inflammatory cytokines, thus facilitating a *PA*-induced cytostorm. Conversely, preventing *PA*- and/or cytokine-induced PDE4B expression by genetic ablation in mice, or siRNA-mediated PDE4B knockdown in cell culture, alleviates the synergistic production of primary and secondary response cytokines, and protects mice from acute lung injury. Despite dampening the host innate immune response, PDE4B deficiency improves bacterial clearance in mice for two reasons: (1) the hyper-elevated levels of proinflammatory cytokines induced by *PA* infection, classically defined as the cytostorm, are actually unnecessary to generate an effective immune response, such as the recruitment and activation of immune cells to/at the site of infection; and (2) the hyper-elevated levels of cytokines do, however, significantly impair bacterial clearance, because they moonlight as cryogens and induce substantial hypothermia in the animals. Taken together, this study identifies PDE4B as a suitable therapeutic target for *PA*-induced lung injury.

2. MATERIALS AND METHODS

2.1. Animals

PDE4B knockout mice[10] were generated by Drs. S.-L. Catherine Jin and Marco Conti (Stanford University, CA) and kindly distributed *via* the Mutant Mouse Resource and Research Centers (MMRRC) of the University of California at Davis. The mice were maintained on a C57BL/6 background by Het/Het breeding and PDE4B knockout mice are compared to their wildtype littermates. The genotypes of the mice were assessed twice by PCR (the first time prior to weaning; the second time, using a new tissue sample for DNA isolation, after the animal was used in an experiment and euthanized) using the following three primers: 1. Wildtype forward primer: 5’-CAAGTCCTTGGAATTGTATCG-3’; 2. Knock-out forward primer: 5’-CTAAAGCGCATGCTCCAGACTG-3’; 3. Common reverse primer: 5’-GCCCATGAATTAAACAGCAG-3’ (see Supplementary Fig. S1A). In line with prior reports revealing a role of PDE4B that is restricted to specific subcellular compartments (or microdomains of cAMP signaling)[14–16], ablation of PDE4B does not produce a significant increase in global, baseline cAMP levels (Supplementary Fig. S1C), nor trigger compensatory changes in the expression of other PDE4 subtypes (Supplementary Fig. S1B), in lung tissue. The animals were group-housed four mice per cage with *ad libitum* access to food and water and were maintained in a temperature-controlled (22–23°C) vivarium with a 12-h light/dark cycle. Adult mice ≥10 weeks of age and of either sex were used for experimentation by dividing cage littermates into experimental groups. Experimenters were blinded to the genotype of the animals and the treatments they received until data acquisition and analyses were completed. All experiments and procedures were conducted in accordance with the guidelines described in the Guide for the Care and Use of Laboratory Animals (National Institutes of Health, Bethesda, MD, USA) and were approved by the University of South Alabama Institutional Animal Care and Use Committee.

2.2. Infection of mice with *Pseudomonas aeruginosa,* bronchoalveolar lavage, blood and lung collection, and determination of bacterial load

Pseudomonas aeruginosa (*PA*) strain *PA01* was a gift from Dr. Cindy Tran (University of California San Francisco, CA). The bacteria were grown on Luria Bertani agar overnight and subsequently suspended in PBS. An inoculum of 5×10^6 CFU in 50 μl of PBS was used for intranasal infection of mice under isoflurane anesthesia as described[17]. Mice were euthanized 16 hours post infection with an overdose of pentobarbital followed by cardiac puncture, broncho-alveolar lavage (BAL), extraction of the right lung, and formalin-fixation and extraction of the left lung. Blood from cardiac punctures was collected in serum separator tubes (Becton/Dickinson, Franklin Lakes, NJ), the serum was separated following the manufacturer's instructions, and the resulting serum samples were frozen at −80°C until measurement of cytokine levels. Broncho-alveolar lavage fluid (BALF) was collected by flushing the lungs three times each with 0.8 ml of PBS containing 2% bovine serum albumin (BSA) and a protease inhibitor cocktail (Complete inhibitor cocktail, Roche, Mannheim, Germany). After removal of a 200 μl aliquot of the original BALF to determine bacterial titers, BALF samples were then centrifuged at 400 × g and the supernatants were stored at −80°C until measurement of cytokine levels. The BALF cell pellets were processed for cell count and flow cytometry as described below. The right lung lobes were extracted and homogenized in 1 ml of PBS containing protease inhibitors (Complete inhibitor cocktail, Roche, Mannheim, Germany) using a Dounce glass homogenizer. After removal of a 200 μl aliquot to determine bacterial titers, the remaining lung homogenates were frozen at −80°C until measurement of cytokine levels. The left lung lobes were inflation-fixed, extracted, and submerged in 10% neutral buffered formalin (ThermoFisher Scientific, Waltham, MA) until processing. Fixed lungs were embedded in paraffin, sectioned, and stained with hematoxylin and eosin (H&E). To determine bacterial titers in BALF or lung homogenate, serial dilutions of these samples were spread on Luria Bertani agar plates and the number of bacterial colonies was counted the next day following overnight incubation of the plates at 37°C.

2.3. Measurement of core body temperature

Body temperature was measured using a thermocouple thermometer (MicroTherma 2T) with mouse rectal probe (RET-3), both from Braintree Scientific (Braintree, MA).

2.4. Flow cytometry analysis of immune cell types in BAL fluid

BALF cells were collected *via* a 10-minute centrifugation at 400 × g. After removal of the BALF supernatant, cells were resuspended in 100 μl of ice-cold lysis buffer (150 mM NH_4Cl, 10 mM $KHCO_3$, 0.1 mM EDTA, pH 7.2) for 5 min on ice to lyse red blood cells, followed by addition of 2 ml of ice-cold PBS. After centrifugation (10 minutes at 400 × g), supernatants were aspirated, and cells were suspended in 100 μl PBS and total BALF cell count was determined using a hemocytometer. BALF cells were washed once more with PBS and immune cell populations stained using an antibody cocktail comprised of a standard panel of immunophenotyping antibodies including F_c receptor Block and antibodies against CD45, CD11b, Gr1, CD11c, and SiglecF as described previously[18, 19]. Splenocytes were used for compensation controls. Please see Supplementary Figure S2 for a list of the clones, fluorochromes and manufacturers for antibodies used to stain BALF

cells or compensation controls. Population frequencies were obtained by flow cytometry using FACSCanto II and subsequent analysis with FlowJo (BD Biosciences, San Jose, CA), and immune cell populations were enumerated using total cell count in BALF. All immune cell populations were gated as CD45 positive. Neutrophils were identified as Gr1 and CD11b double positive, alveolar macrophages were identified as CD11c and SiglecF double positive, and eosinophils were identified as SiglecF positive and CD11c negative (see Supplementary Fig. S3 for an illustration of the gating approach).

2.5. Lung histopathology

Lung histopathologic scoring was performed on coded lung sections by a pathologist blinded to sample identities by assessing luminal and peri-bronchial inflammation, the number of micro-abscesses (if present), as well as perivascular, interstitial, and alveolar inflammation, as well as pleural thickening. To obtain the luminal and peri-bronchial scores, the airways present in the section were counted and each given an injury score between 0 (least injury) and 3 (severe); the final score represents the average of all airways in the section. Perivascular, interstitial and alveolar inflammation, as well as pleural thickening, were scored similarly by counting and scoring inflamed vessels in the lung section (perivascular) or evaluating inflammation and injury in individual sections with a score between 0 (least) and 3 (worst). Micro-abscesses (clusters of neutrophils in the lung parenchyma) were counted in each lung section and were assigned a score between 0 and 3 as follows: Score 0 = no micro-abscesses; Score 1 = 1–10 micro-abscesses; Score 2 = 11–20 micro-abscesses; Score 3 = 21–30 micro-abscesses. Final scores were obtained by adding scores of individual categories.

2.6. Survival Study and Humane Endpoints

To determine the effect of PDE4B ablation on mortality after intranasal *PA01* infection, the animals' weight and general health were assessed by an experimenter blinded to the genotype of the mice three times a day (7 am, 1 pm and 7 pm) for the first four days post infection, and at least once a day (1 pm) on days five to seven after infection. Pre-defined humane endpoints warranting euthanasia were a >30% reduction in initial body weight, immobility, shaking, loss of equilibrium, or as determined by veterinary staff. We should note that this model produces a characteristic phenotype dubbed spinning[20], or rolling, in which the animal initially presents with a sideways head tilt (see Supplementary Fig. S4), which routinely progresses within a few hours to an increasing and eventually complete loss of balance/equilibrium, and eventually death (likely accelerated by the animal's inability to eat/drink due to its head tilt/imbalance) within a few hours. Hence, mice found with significant head tilt/imbalance were euthanized (humane endpoint = loss of equilibrium) and counted as non-survivors.

2.7. Assessment of lung vascular permeability using Evans Blue Dye extravasation

16 h after intranasal infection with *PA01*, a sterile-filtered Evans Blue Dye (EBD) solution comprising 0.4% EBD (Acros Organics #195550050) and 4% w/v BSA in PBS was administered *via* the lateral tail vein at a dose of 20 mg/kg. 1 h later, mice were sacrificed by EUTHASOL® Euthanasia Solution (Patterson Veterinary, Greeley, CO) injection and lungs were perfused free of blood *via* the right ventricle using 10 ml of sterile PBS. The left

lung was excised, weighed, and subsequently suspended in 1 ml formamide and incubated at 55°C for 18 h to extract the EBD. The EBD concentration in the tissue extract was then measured based on the optical density of the EBD/formamide solution at 620 nm against a standard curve and calculated as the ratio of total EBD over wet weight of the lung tissue.

2.8. Cytokines, ELISA and Western blotting

Cytokine levels in BAL fluid, lung homogenates, and serum were measured using ELISA kits for mouse TNF-α (#7324), IL-1β (#7013), and IL-6 (#7064) from ThermoFisher Scientific (Waltham, MA) or for KC (#DY453) from R&D Systems/BioTechne (Minneapolis, MN). Myeloperoxidase (MPO) levels were measured using an ELISA (#DY3667) from R&D Systems/BioTechne (Minneapolis, MN). Recombinant mouse TNF-α (#Z02918) and IL-1β (#Z02988) were obtained from GenScript (Piscataway, NJ). Serum cytokines were measured using the LEGENDPlex bead array (Mouse inflammation panel, #740150; Biolegend, San Diego, CA) according to the manufacturer's protocol. Antibodies against PDE4B (#SC25812) and β-actin (#SC477778) were from Santa Cruz Biotechnology (Santa Cruz, CA), the antibody against PDE4A from Pierce Biotechnology, Waltham, MA (#PA1–31131), and antibodies against PDE4D from Sigma-Aldrich, St. Louis, MO (#SAB1100525; immunoprecipitation) and Abcam, Waltham, MA (#ab171750; immunoblotting).

2.9. Mammalian cell culture, treatment, and siRNA-mediated knockdown

Immortalized mouse embryonic fibroblast (MEF) cells were a kind gift from Dr. Alan C. Sartorelli (Yale University School of Medicine, New Haven, CT) and the murine macrophage cell line (RAW 264.7) was obtained from ATCC (American Type Culture Collection, Manassas, VA). Cells were maintained in Dulbecco's Modified Eagle Medium (DMEM) containing 10% fetal bovine serum, 30 μg/ml penicillin, and 100 μg/ml streptomycin at 37°C under 5% carbon dioxide. For experiments, cells were generally passaged into 12-well plates at 100,000 (MEFs) or 200,000 (RAW264.7) cells/well and the near-confluent cultures were used two days later for cell treatments and subsequent harvest.

To induce siRNA-mediated knockdown, MEFs and RAW 264.7 cells were reverse-transfected using Lipofectamine RNAi-MAX (Thermo Fisher Scientific, Waltham, MA) following the manufacturer's instructions. In short, first, the siRNA and transfection reagent complexes were prepared in Opti-MEM reduced-serum medium (Thermo Fisher Scientific, Waltham, MA) in 12-well plates and incubated for 20 min at room temperature, after which cells and complete media were added on top. The siRNA against PDE4B (5′-CAAUGUGGCUGGGUACUCAtt-3′; #PDSIRNA2D SASI_Mm01_00054410) as well as the control-siRNA (#SIC001, siRNA Universal Negative Control #1) were obtained from Sigma-Aldrich (St. Louis, MO). Two days after cell seeding/transfection, cells were washed once with phosphate-buffered saline (PBS) and then maintained in 500 μl of serum-free DMEM. Cells were then treated with *P. aeruginosa* lipopolysaccharide (*PA*-LPS), TNF-α, IL-1β, or a combination of TNF-α and IL-1β at the concentrations indicated, and media was collected 6 h later to measure levels of released cytokines, whereas the cells were harvested to measure protein content or perform Western blotting.

2.10. Immunoprecipitation (IP) and PDE activity assay

Tissues were homogenized in buffer containing 20 mM HEPES (pH 7.4), 1 mM EDTA, 0.2 mM EGTA, 150 mM NaCl, 20% sucrose, 1 μM microcystin-LR, complete protease inhibitor cocktail (Roche Diagnostics, Indianapolis, IN, USA), and 1% Triton X-100. After a 30-min rotation at 4°C, cell debris was pelleted with a 10-min centrifugation at 20,000 × g, and equal amounts of protein of the resulting extracts were subjected to IP using 30 μl Protein G Sepharose and 2 μg of PDE4B antibody (#SC25812, Santa Cruz Biotechnology, Santa Cruz, CA) or normal rabbit IgG as a control. After incubation for 3 h at 4°C, the resin was washed 3 times and proteins recovered in the IP pellets were detected by PDE activity assay as described previously[21], with minor modifications. In short, samples were assayed in a reaction mixture of 200 μl containing 40 mM Tris/HCl (pH 7.4), 10 mM $MgCl_2$, 1.34 mM 2-mercaptoethanol, 1 μM cAMP, and 0.1 μCi [^{3}H]cAMP (Perkin Elmer, Waltham, MA) for 20 min at 37°C followed by heat inactivation in a boiling water bath for 1 min. The PDE reaction product, 5'-AMP, was then hydrolyzed by incubation of the assay mixture with 50 μg of *Crotalus atrox* snake venom (Sigma-Aldrich, St. Louis, MO) for 20 min at 37°C, and the resulting adenosine was separated by anion-exchange chromatography on 1 ml of AG1-X8 resin (Bio-Rad Laboratories, Hercules, CA) and quantitated by scintillation counting.

2.11. Statistical analysis

Unless indicated otherwise, data are expressed as the mean ± SEM. The Mann-Whitney test was used to compare means of two groups in animal experimentation. One-way ANOVA was used for the analysis of cell culture experiments, and 2-way ANOVA with Tukey's multiple comparison test was used for analyses of time-courses. Kaplan-Meier survival curves were compared using Mantel-Cox log-rank test. Differences were considered significant if $p<0.05$. Analyses were performed using Prism 8 software (GraphPad Software, San Diego, CA).

3. RESULTS

3.1. Ablation of PDE4B protects from *Pseudomonas aeruginosa (PA)*-induced inflammation and lung injury in mice.

To assess the role of PDE4B in *PA*-induced acute lung injury, PDE4B-knockout (4BKO) mice and wildtype (4BWT) littermate controls were infected intranasally with 5×10^6 CFU of the *PA* lab strain *PA01,* a dose that produces ~50% of 7-day mortality in this model[17]. Sixteen hours later, the animals were subjected to broncho alveolar lavage (BAL), the right lung was extracted and homogenized to determine cytokine levels, bacterial load and PDE4B activity, whereas the left lung was inflation-fixed and processed for tissue sectioning. As shown in Fig. 1A/B and Supplementary Fig. S6, infection with *PA01* induces inflammation throughout all segments of the lung including luminal, peri-bronchial, perivascular, parenchymal and alveolar spaces. Exposure of cells to pathogen-associated molecular patterns (PAMPs), such as *E. coli*-LPS, has been shown to induce PDE4B expression in response to TLR4 activation[10]. Similarly, infection with *PA01* increases PDE4B activity in the lungs of WT mice (Supplementary Fig. S5). Genetic ablation of PDE4B exerted several protective effects in the animals, including reduced lung

inflammation, as determined by histopathologic scoring of lung sections (Fig. 1B), an effect that was mainly driven by a reduction in luminal, interstitial and alveolar inflammation, and a reduction in the number of abscesses representing neutrophil clusters observed throughout the lung parenchyma (please see Supplementary Fig. S6). Ablation of PDE4B in mice was associated with a significant reduction of several pro-inflammatory cytokines, including TNF-α, IL-1β, IL-6, and KC, in broncho-alveolar lavage fluid (BALF) (Fig. 1C–F) and/or right lung tissue homogenates (Supplementary Fig. S7) of *PA01*-infected animals. Lung infection with *PA01* also associates with significant systemic inflammation, as indicated by increased levels of pro-inflammatory cytokines in the serum of infected animals. However, mice deficient in PDE4B exhibited reduced systemic inflammation as indicated by reduced levels of pro-inflammatory cytokines, including TNF-α and IL-6, in serum (Supplementary Fig. S8). Bacterial lung infection is well established to induce airway neutrophilia, and this is reflected by a substantial increase in the number of neutrophils in BALF of *PA01*-infected mice. Interestingly, despite the reduction in the levels of pro-inflammatory cytokines that mediate activation and chemotactic migration of circulating immune cells into the lung (Fig. 1C–F), the total number of leukocytes, as well as the number or frequency of immune cells, including neutrophils, recruited into the airway of 4BKO mice, was similar to that of their WT littermates (Fig. 1G–J and Supplementary Fig. S9). In the same vein, the levels of myeloperoxidase (MPO), a measure of neutrophil recruitment and activation, were also unchanged in BALF of 4BKO and WT littermates (Fig. 1K). The observation that luminal inflammation is reduced in 4BKO mice (Supplementary Fig. S6), whereas the number of recovered BALF cells is not (Fig. 1G/H), may suggest that PDE4B ablation reduces the number of immune cells that are attached to the airway surface (and not recovered by BAL), whereas the number of immune cells moving freely within the airway is unaltered. Severe lung infection/inflammation can produce pulmonary vascular dysfunction and permeability, leading to edema. To explore the role of PDE4B in this paradigm, we assessed the extravasation of Evans Blue Dye (EBD), delivered *via* tail vein injection at 16 h post infection, into the lung parenchyma as a readout of vascular leakage. As shown in Fig. 1L, *PA01*-infection induced a significant increase in EBD leakage in WT mice compared to uninfected controls, and this effect was alleviated in 4BKO mice. Finally, as shown in Fig. 1M, ablation of PDE4B improves the 7-day survival rate of mice upon intranasal *PA01*-infection. Taken together, these data suggest that genetic ablation of PDE4B in mice is effective in ameliorating hyperinflammatory responses, lung injury and mortality upon acute *P. aeruginosa* lung infection.

3.2. Mice deficient in PDE4B exhibit improved bacterial clearance.

For infectious diseases, it is critical that therapeutic approaches which dampen the body's immune response, do not diminish the efficacy of clearance of the pathogen. This is a particularly pressing issue for *P. aeruginosa* lung infections, as this pathogen has evolved multiple effector mechanisms to evade immune detection and clearance[22, 23], and exhibits high rates of multi-drug resistance[24]. We thus wished to confirm that the observed anti-inflammatory effects of PDE4B ablation (Fig. 1), do not result in increased bacterial loads in the animals, particularly given that such an effect was recently reported in *PA01*-infected mice treated with high doses of the PAN-PDE4 inhibitor Roflumilast[17]. To this end, the number of live bacteria in BALF and lung tissue of 4BWT and 4BKO mice was determined

by plating serial dilutions of the samples. Unexpectedly, not only was the bacterial load in 4BKO mice not increased, but we observed a significant reduction in the bacterial load in lung tissue (Fig. 2A) and BALF (Fig. 2B) of 4BKO mice compared to WT littermate controls. This observation prompted a series of experiments to explore why and how PDE4B ablation may alleviate immune responses, while at the same time enhancing bacterial clearance.

In humans as well as mice, exposure to low levels of pathogens or pathogen-associated molecular patterns (PAMPs), such as LPS, induces fever. Conversely, upon exposure to high doses of pathogens or PAMPs (such as those that produce mortality), mice develop hypothermia, similar to critically ill patients that often cycle through periods of intermittent fever and hypothermia[25–28]. In this context, we noted that WT mice infected with *PA01* underwent substantial hypothermia, starting within 2 h after infection, which reached a maximal decrease in body temperature of up to −10°C within 6 h, followed by a slow return to baseline body temperature (Supplementary Fig. S10). Intriguingly, compared to their WT littermates, mice deficient in PDE4B were less hypothermic throughout the entire time course (Fig. 2C and Supplementary Fig. S10).

3.3. Ablation of PDE4B protects mice from *PA*-induced hypothermia, and thereby improves bacterial clearance.

To determine whether improved bacterial clearance in PDE4B-KO mice is causally connected to infection-driven hypothermia, and if so, whether improved clearance is a cause or a consequence of alleviated hypothermia, we tested whether easing hypothermia in mice *via* external heat would also improve bacterial clearance in mice. To this end, we compared immune responses and bacterial clearance in WT mice kept at room temperature (RT; ~22°C) to mice whose cages were placed on heating mats set to 33°C immediately after *PA*-infection. Notably, the animals' behaviors during these experiments suggest that hypothermia is a significant stressor on the mice and that the animals attempt to alleviate this with heat-seeking behaviors. *PA*-infected mice kept at ambient temperature (RT) assume balled-up postures, thus reducing body surface and associated heat loss, and are consistently found in huddles (Fig. 3A, left picture), suggesting they attempt to mitigate hypothermia by sharing body heat. Conversely, mice placed on heating mats consistently spread out away from each other and appear to flatten out on the cage bottom, thus increasing their surface area that is in contact with the heat source - the heating mat underneath the cage bottom (Fig. 3A, right picture). Clearly, absorbing external heat through the cage bottom is a more effective approach for maintaining body temperature, compared to balling up and huddling, and thus predominates the behavioral response of mice on the heat mat. Indeed, the core body temperature of mice on heat mats is protected from the substantial hypothermia observed in mice kept at RT (Fig. 3B). By limiting hypothermia, external heat significantly improved bacterial clearance, as live bacteria in both BALF and lungs of mice placed on heat mats were significantly lower than those of mice kept at room temperature (Fig. 3C and Supplementary Fig. S11A). In a pattern comparable with the effect of PDE4B ablation, the levels of pro-inflammatory cytokines, including TNF-α, IL-1β, IL-6 and KC, were significantly reduced in BALF (Fig. 3D–G), lung (Supplementary Fig. S11B–E) and serum (Supplementary Fig. S12) of mice placed on heat mats compared to RT controls. Conversely,

the number of immune cells in BALF (Fig. 3H), including neutrophils (Supplementary Fig. S13), was not reduced by placing mice on 33°C heat mats (if anything, there is a subtle increase in the number of BALF cells in mice placed on 33°C heat mats, compared to RT controls; Fig. 3H and Supplementary Fig. S13). Finally, placing cages on a 33°C heat mat also improved 7-day survival compared to mice kept at RT (Fig. 3I), replicating a phenotype reminiscent of the effects of PDE4B ablation.

The experiments above demonstrate that minimizing hypothermia, such as *via* external heating, significantly improves bacterial clearance in *PA01*-infected mice. This begs the question of whether diminished hypothermia is indeed the cause of the improved bacterial clearance in PDE4B-KO mice compared to their WT littermates. To test this, both PDE4B-KO and WT mice were placed on heating mats after *PA01*-infection. This ablated the difference in core body temperatures between the two groups (Fig. 3J). At the same time, we no longer observed a significant difference in the bacterial load in BALF (Fig. 3K) and lungs (Supplementary Fig. S14) between PDE4B-KO and WT mice, suggesting that the alleviated hypothermia in PDE4B-KO mice is the cause of their improved bacterial clearance. In line with this idea, under the controlled temperature conditions of *in vitro* experiments (e.g. 37°C), ablation of PDE4B does not affect the efficiency of phagocytosis as shown previously[29], and does not affect the efficiency of bacterial killing (see Supplementary Fig. S15).

3.4. Critical role of pro-inflammatory cytokines acting as cryogens in *PA*-induced hypothermia.

Having established that alleviating hypothermia is responsible for the improved bacterial clearance in PDE4B-KO mice, we then wished to explore how ablation of PDE4B mediates its effects on hypothermia. A significant number of the cytokines produced during the innate immune response, including TNF-α, IL-1β and IL-6, serve not only to recruit immune cells to the site of infection and activate them, but also play critical roles in body temperature regulation after their release into the systemic circulation. At low levels, these cytokines produce fever, whereas at high levels, such as those produced by exposure to high doses of LPS and/or bacteria, they have been shown to drive hypothermia[25, 27, 28, 30]. Given that *PA01*-infection dramatically increases the levels of several of these acute-phase cytokines, in particular TNF-α and IL-1β (Fig. 1C and Supplementary Figs. S7 and S8), and that PDE4B ablation is well-established to alleviate TNF-α production in response to TLR4 activation[10] (also see reduction in TNF-α in *PA01*-infected PDE4BKO mice; Fig. 1C and Supplementary Figs. S7A and S8A), we thus explored the idea that the reduction in these acute-response cytokines represents the mechanism whereby PDE4B ablation alleviates *PA*-induced hypothermia and improves bacterial clearance. To test the role of these cytokines in body temperature regulation directly, mice were injected with TNF-α or IL-1β and their body temperature was measured over the following 8 h (Fig. 4A). In line with prior studies[31], injection of either of these cytokines produced a significant reduction in body temperature, with the effect of IL-1β being immediate (apparent at 1 h after injection), whereas the effect of TNF-α is slower in onset (~5 h after injection), likely reflecting a requirement for changes in gene expression. Still, the level of hypothermia induced by either TNF-α or IL-1β (−1 to −2°C) is minor compared to the substantial hypothermia

associated with *PA01* infection (Fig. 2C). However, as shown in Fig. 4A, we find that the simultaneous injection of both cytokines acts synergistically to induce substantial hypothermia in mice. The synergistic action of TNF-α and IL-1β on body temperature is paralleled by a synergistic induction of serum IL-6 levels, which has been shown to be a master regulator of cytokine-mediated fever and/or hypothermia in settings of infection[25, 28].

Surprisingly, mice deficient in PDE4B are still partially protected from hypothermia induced by the injection of TNF-α and IL-1β (Fig. 4C), as well as the synergistic induction of IL-6 by this cytomix (Fig. 4D). These data suggest that, in addition to the well-established role of PDE4B in gating the LPS/TLR4-induced production of TNF-α[10, 11], PDE4B also regulates inflammatory signaling downstream of TNF-α and/or IL-1β, specifically the TNF-α/IL-1β-dependent induction of IL-6 and its associated hypothermia.

3.5. Ablation of PDE4B alleviates the cytostorm acting both upstream and downstream of TNF-α and IL-1β.

We next aimed to confirm that PDE4B acts downstream of TNF-α and IL-1β in a simplified system, and particularly in the absence of the changes in body temperature that are necessarily associated with animal studies. To this end, we explored the role of PDE4B in cell culture systems. In line with prior reports showing that *E. coli*-LPS induces the expression of PDE4B in mouse peritoneal macrophages[10], treatment of RAW264.7 mouse macrophages, while expressing little to no PDE4B at baseline, substantially increased PDE4B expression in response to *PA*-LPS (Fig. 5A). Preventing *PA*-LPS-induced PDE4B expression *via* siRNA-mediated knockdown significantly reduced TNF-α production (Fig. 5B). In addition, the siRNA-mediated knockdown of PDE4B also reduced *PA*-LPS-induced IL-6 production (Fig. 5C). IL-6 is considered a secondary-response gene that can be induced by signaling of acute-response cytokines such as TNF-α and IL-1β (see Fig. 4B). To exclude the possibility that the reduction in IL-6 levels is simply a reflection of the PDE4B-siRNA-mediated reduction of TNF-α in the cell culture media, we then exposed RAW264.7 macrophages to exogenous TNF-α and/or IL-1β. However, neither treatment by itself, nor their combination, produced a significant induction of PDE4B expression (Supplementary Fig. S16), nor did it induce IL-6 expression, suggesting that RAW264.7 macrophages do not effectively respond to TNF-α/IL1β without PAMP-induced priming. We thus utilized mouse fibroblasts, a cell type that is now well-recognized as playing critical roles in the immune response and is also expected to respond to TNF-α/IL-1β[32]. As shown in Fig. 5D, mouse embryonic fibroblasts (MEFs) showed the sought-after properties and induced PDE4B expression after exposure to TNF-α alone, which was further increased in the presence of IL-1β (Fig. 5D). Treatment with TNF-α also triggered a significant production of IL-6, which was further enhanced by co-treatment with IL-1β (Supplementary Fig. S17). Transfection of MEFs with siRNA against PDE4B effectively prevented TNF-α/IL-1β-induced PDE4B expression (Fig. 5E), and in addition, significantly alleviated IL-6 production in response to TNF-α alone (Supplementary Fig. S17B) or the combination treatment with TNF-α and IL-1β (Fig. 5F). Taken together, these data confirm that in addition to being induced by PAMPs, such as LPS, expression of PDE4B is synergistically induced by signaling of acute-response cytokines, such as TNF-α and IL-1β, and enhances their downstream signaling by removing the negative restriction mediated by intracellular

cAMP on the production of pro-inflammatory cytokines (Fig. 5G). Thus, inactivation of PDE4B exerts independent constraints on the induction of acute-response cytokines, as well as their downstream signaling, for example the induction of secondary-response cytokines such as IL-6, and thereby impairs the perpetuation of the *PA*-induced cytostorm in cells and animals alike (Fig. 5H).

4. DISCUSSION

4.1. PDE4B as a potential therapeutic target to alleviate the *P. aeruginosa*-induced cytostorm and lung injury.

Targeting individual PDE4 subtypes is a promising approach to separate the therapeutic benefits of PAN-PDE4 inhibitors, such as their broad anti-inflammatory properties, from their class-defining, dose-limiting side effects, in particular nausea and emesis[5, 7, 9]. To this end, PDE4B has been proposed as a target for the development of subtype-selective PDE4 inhibitors, given that the genetic ablation of PDE4B in mice recapitulates some of the anti-inflammatory properties of PAN-PDE4 inhibitors, including a reduction of TNF-α production upon exposure of cultured peritoneal macrophages to *E. coli*-LPS, or a delay in the migration of leukocytes into the airway upon LPS inhalation in mice[11, 29]. Using the latter model, ablation of PDE4D also exerted a pattern of anti-inflammatory effects distinct from that of PDE4B, and may thus also represent a target for drug development[29]. Conversely, ablation of PDE4A in mice did not produce any benefits in this LPS-lung injury model[29] and ablation of PDE4C has not been explored thus far. Our current study confirms and extends the evidence identifying PDE4B as a promising drug target for inflammatory diseases in several directions.

First, we extend prior findings in non-infectious/LPS models[13, 29] to show that ablation of PDE4B protects mice from lung inflammation and injury caused by a live pathogen, *P. aeruginosa*, that is infamous for having evolved multiple virulence mechanisms to prevent detection and clearance by the host's immune system (Fig. 1)[22, 23]. Moreover, *P. aeruginosa* exhibits high rates of multi-drug resistance, thus, effective clearance of the infection with antibiotics is not a given in the clinical setting[24]. In this context, it is important to note that PDE4B is not essential for any facet of the host immune response; instead, the amount of PDE4B in the host cell "only" gates the intensity of the immune response. For example, despite the complete and systemic ablation of PDE4B in the KO mice, all pro-inflammatory cytokines studied here (TNF-α, IL-1β, IL-6, KC) are still produced, though at lower levels, in response to *PA*-infection (Fig. 1C–F). As a result, inactivation of PDE4B can alleviate hyperinflammatory responses without being immunosuppressive, and thus without worsening the bacterial infection. Despite reducing the levels of lung- and systemic pro-inflammatory cytokines, ablation of PDE4B does not reduce the number of total leukocytes or neutrophils recruited into the airway at 16 hours post infection (Fig. 1G–K), which may represent one safeguard against increased bacterial load (Fig. 2A/B). Or, put differently, our findings suggest that the high levels of cytokines classically described as the cytostorm, are not actually necessary to muster an effective immune response and may instead be counterproductive for bacterial clearance given their cryogenic effects (Fig. 5G/H).

Second, an attractive feature of targeting PDE4B therapeutically is that the specific protein variant involved in the regulation of innate immune responses, PDE4B2, is not constitutively expressed in the host's cells, and is instead acutely induced upon detection of pathogen-associated molecular patterns (PAMPs), such as LPS, by the host's immune and non-immune cells[10] (Fig. 5A/D/E). Thus, a PDE4B-selective inhibitor would exert selective efficacy only in cells that are both presently and actively involved in the innate immune response, and thus express PDE4B, while the drug would not have a biologic effect in other cells, given the absence of its molecular target. Importantly, we show here that PDE4B/PDE4B2 expression is not just induced by the LPS-dependent activation of TLR4 reported previously[10] (Fig. 5A), but also downstream of signaling by the acute-response cytokines TNF-α and IL-1β (Fig. 5D/E, Supplementary Fig. S16). The efficacy of a PDE4B-selective inhibitor would thus extend to both cells exposed to PAMPs as well as cells that induce PDE4B2 expression in response to local or systemic exposure to acute-response cytokines. The unique efficacy of PDE4B inactivation in alleviating the cytostorm is thus rooted in two synergistic aspects: 1. its simultaneous "upstream" and "downstream" effect on both the production of TNF-α itself (Fig. 5B), as well as the TNF-α-mediated induction of secondary response cytokines, such as IL-6, which we demonstrate in both mice (Fig. 4D) and cell culture models (Fig. 5F and Supplementary Fig. S17B); and 2. the disruption of the interplay between TNF-α and IL-1β in synergistically inducing PDE4B to promote the induction of secondary response cytokines, which we demonstrate in both cells (Supplementary Fig. S16A) and mice (Fig. 4B).

While alleviating the acute inflammatory response to bacterial infection *per se* may explain the main therapeutic benefits resulting from PDE4B ablation, we cannot exclude the possibility that PDE4B ablation may exert benefits *via* additional avenues, such as improving survival by promoting repair and healing processes after the bacteria have been cleared. Indeed, elevated cAMP signaling in general, and treatment with PAN-PDE4 inhibitors in particular, is well established to induce a number of pro-resolving molecules and pathways[33–35], and the potential role of PDE4B in mediating some of these effects remains to be elucidated.

Third, our study sheds light on the fact that by modulating the systemic levels of several pro-inflammatory cytokines, which in addition to their classical role in the recruitment and activation of leukocytes, may also act as pyrogens or cryogens[25, 27, 28], targeting PDE4/PDE4B may also affect central body temperature regulation with potentially critical impact on health outcomes. Indeed, how a PDE4 inhibitor-induced suppression of pro-inflammatory cytokines exerts therapeutic benefits may potentially depend in part on whether the injury is due to microbial infection or due to sterile/non-infectious inflammation. For example, acute-response cytokines such as TNF-α may contribute to endothelial and epithelial barrier dysfunction, and hence vascular leakage and edema. For this facet of cytokine function, targeting PDE4/PDE4B may exert beneficial, barrier-protective effects (see Fig. 1L) independent of whether the cause of injury is infectious in nature or not. However, acute-response cytokines also promote recruitment of leukocytes, and their production/release of various agents to destroy invading pathogens (including proteases/elastase or reactive oxygen species), but that can also damage the host. While there is no apparent downside to alleviating this "clearance/killing" facet of cytokine action by targeting PDE4/

PDE4B in settings of non-infectious injury (e.g. trauma), it is critical to maintain the effective clearance of the pathogen in settings of bacterial infections, in particular if the efficacy of antibiotic treatment is not guaranteed[24]. In this context, it is important to note that while prior studies have shown a delay in LPS-induced leukocyte infiltration into the airways of PDE4B-KO mice during the early hours of infection[29], we find that at 16 h after *PA*-infection, similar levels of leukocytes (Fig. 1G–I) and myeloperoxidase (Fig. 1K) are found in BALF of PDE4B-KO mice and WT controls. Finally, the effects of acute-response cytokines on body temperature may have opposite effects on outcomes, depending on whether inflammation is due to infection or not. In settings of sterile/non-infectious inflammation, alleviating a cytokine-driven fever may be beneficial, given that all the body's systems are attuned to optimal function at a constant temperature of ~37°C. Conversely, in settings of infection, fever can be beneficial and is thought to improve microbial clearance, particularly if the increase in body temperature can be tolerated by the host, but exceeds the microbe's optimal growth temperature[36]. Hypothermia on the other hand, can provide benefits in settings of sterile/non-infectious injury, such as by slowing down metabolism, reducing the production of reactive oxygen species and apoptosis, or a literal "cooling down" of inflammatory responses. Artificially-induced, often locally-applied hypothermia is thus pursued as a therapeutic approach, such as for brain or spinal cord injuries[37]. However, our study shows that hypothermia in settings of *PA*-lung infection in mice is detrimental, as it is associated with an increased bacterial burden (Fig. 2A/B), and that preventing hypothermia with external heating (Fig. 3) or by alleviating the *PA*-induced cytostorm by genetic ablation of PDE4B (Fig. 1C–F and Supplementary Fig. S8) improves bacterial clearance, and thereby overall outcomes. The idea that hypothermia would be maladaptive in settings of bacterial lung infection aligns well with the conclusions of a recent meta-analysis suggesting that therapeutic hypothermia in humans, while not increasing the overall risk of infection, selectively increased the risk of pneumonia and sepsis[38].

Fourth, using a similar infection/injury model, a recent report showed that treatment with high doses of the PAN-PDE4 inhibitor Roflumilast resulted in increased bacterial growth and dissemination, as well as increased mortality, upon acute lung infection with *PA01*[17], in contrast to the improved survival of mice deficient in PDE4B that we report here (Fig. 1M). This is not a Roflumilast-specific effect, but appears to be a class-effect of PAN-selective PDE4 inhibitors. Prior studies reported increased mortality and impaired bacterial clearance also upon prophylactic treatment with the PAN-PDE4 inhibitor Rolipram in a *Klebsiella pneumoniae* lung infection model[39]. In addition, in a *Streptococcus pneumoniae* lung infection model, Rolipram also did not improve bacterial clearance or mortality (though neither did Rolipram worsen bacterial load and/or mortality)[40]. Finally, in our own hands, treatment of wildtype mice with Rolipram also trends to increase (rather than decrease) mortality in *PA01*-infected mice (Supplementary Fig. S18B).

While infrequent, the observation that PAN-PDE4 inhibition does not phenocopy the effects of inactivating a single PDE4 subtype has been reported previously in a study exploring the roles of PDE4s *via* the siRNA-mediated knockdown of PDE4B and/or PDE4D in cell culture[16]. This proved to be because PDE4B and PDE4D controlled spatially distinct cAMP pools that had opposing effects upon the functional readout: the nuclear translocation of DNA-protein kinase (DNA-PK). This opens the possibility that, at the molecular or

cellular level, some of the effects of PDE4B ablation may be functionally counteracted by inactivation of one (or all) of the three other PDE4 subtypes, an option that remains to be explored in the future.

Although the exact cause(s) of their opposing outcomes remains to be determined, there are several noteworthy differences in the phenotypes generated by PAN-PDE4 inhibitor treatment compared to genetic PDE4B ablation. For example, pre-treatment of mice with PAN-PDE4 inhibitors *per se* induces significant hypothermia in mice (Supplementary Fig S18A; please also see[41]), whereas naïve PDE4B-KO mice are normothermic (see 0 h time point in Supplementary Fig. S10). Moreover, while selective ablation of PDE4B alleviates infection-induced hypothermia, treatment with PAN-PDE4 inhibitors does not (see Supplementary Fig. S18A). As another difference between the selective ablation of PDE4B and PAN-PDE4 inhibition, treatment with Roflumilast significantly reduced the number of leukocytes/neutrophils in the airways of mice at 16 h post infection as reported previously[17], whereas ablation of PDE4B does not (Fig. 1G/H). This may suggest that PAN-selective inhibition of PDE4 exerts effects on neutrophil functions (e.g. on chemotaxis, vascular/endothelial attachment, transmigration or bacterial killing) that are not reproduced by selective ablation of PDE4B, but are detrimental to an effective bacterial clearance. In addition, although Roflumilast treatment reduced the levels of several cytokines, such as TNF-α, it actually increased the levels of IL-6. Conversely, ablation of PDE4B leads to a reduction of IL-6 levels in lung and serum (Supplementary Fig. S7/8). Given the critical role of IL-6 in mediating hypothermia (Fig. 4A/B) and the detrimental effect of hypothermia on bacterial clearance and survival in this *PA*-lung infection model (Fig. 2/3), one may speculate that Roflumilast treatment may have perpetuated IL-6-dependent hypothermia and associated morbidity/mortality. Altogether, these differences suggest that while high doses of a PAN-PDE4 inhibitor may exert immunosuppressive effects, selective ablation of PDE4B does not, and is thus a preferential anti-inflammatory approach for the treatment of infectious diseases. Furthermore, treatment with high doses of PAN-PDE4 inhibitors induces a number of acute physiologic effects in mice, including hypothermia, hypokinesia, or increased gastric retention[41, 42], that may reflect an acute/temporary impairment of central autonomic nervous system regulations, and may have acted as an additional insult (2nd hit) during *PA*-infections, leading to worse outcomes, independent of the effects of PDE4 inhibition on the immune response. Importantly, none of the effects are replicated by selective ablation of PDE4B in mice. That PAN-PDE4 inhibitor treatment *per se* induces hypothermia in the absence of bacterial infection and independent of the production/signaling of cytokines (onset of PDE4 inhibitor-induced hypothermia occurs within minutes) is a curious coincidence, given the critical role of PDE4B ablation in alleviating hypothermia mediated by acute-response cytokines we report here, but may nevertheless serve to underscore the importance of body temperature regulation for health outcomes in this *PA*-lung infection model. Treatment with PAN-PDE4 inhibitors, but not ablation of PDE4B, has also been shown to potentiate the anesthetic effects of Isoflurane, and may thereby artefactually augment the delivery of bacteria into the lungs of mice upon intranasal infection under Isoflurane anesthesia[43]. Taken together, based on the opposing effects of high dose-PDE4 inhibitor treatment ([17, 39, 40], and Supplementary Fig. S18) and PDE4B ablation (Fig. 1) in this acute lung injury model, it is tempting to speculate that

selectively targeting PDE4B may not just be equally effective, but may in fact be the more effective therapeutic approach for treatment of acute *P. aeruginosa* lung infections, compared to non-selective PDE4 inhibition. As pointed out earlier, a caveat to this conclusion is that PAN-PDE4 inhibition may produce more effective anti-inflammatory benefits, such as the reported suppression of neutrophil infiltration[17] or the induction of pro-resolving mediators[33, 34, 40], compared to PDE4B ablation, in settings of lung injury in which any impact of a live pathogen can be excluded, such as in settings of sterile inflammation or if PDE4 inhibitors are administered in conjunction with effective antibiotic therapies[40].

Finally, targeting PDE4 for any indication has long been hampered by the narrow therapeutic window of PAN-PDE4 inhibitors, which is defined by nausea and emesis. Given that individual PDE4 subtypes exert unique and non-overlapping physiologic roles, development of subtype-selective inhibitors has long been proposed as an approach to separate therapeutic and adverse effects[7]. While the potential adverse effects of PDE4B-selective inhibitors have not been explored in humans, it is important to note that genetic ablation of PDE4B or treatment with PDE4B-selective inhibitors does not induce some of the correlates used to assess the emetic potential of PDE4 inhibitors in animals, including the induction of gastric retention[42, 44] or shortening the duration of Ketamine/Xylazine-induced anesthesia[45]. Thus, targeting PDE4B may represent a promising approach for development of subtype-selective PDE4 inhibitors with an improved safety profile.

4.2. *P. aeruginosa*-associated hypothermia – dysfunction or regulated response?

In mammals and other homeotherms, body temperature regulation is a complex and tightly regulated process involving integration of multiple behavioral and autonomic nervous system responses, and a large number of effector organs that serve to generate (shivering and non-shivering thermogenesis) or dissipate (cutaneous vasodilation, sweating) heat[30, 46]. Under most environmental conditions, these serve to maintain body temperature within a narrow range (generally around 37°C) to protect vital cellular and physiological functions. However, similar to humans, mice respond to low-level infection/inflammation, such as exposure to low doses of LPS/bacteria, with an increase in body temperature, the fever response. Principally, fever is thought to improve clearance of the causative pathogens by enhancing innate and acquired immune defense mechanisms, and because fever may reach temperatures above the optimal growth conditions for some microorganisms[25]. The latter does not apply to *P. aeruginosa*, however, which grows well at up to 42°C[36].

However, small mammals with a high surface-to-volume ratio, such as mice, expend a substantial portion of their food calories on maintaining body temperature or, in case of infection, generate fever. In settings of severe infection/inflammation, such as upon administration of high doses of LPS or bacteria, or for instance the lethal doses of *PA01* used in the present study, mice instead undergo hypothermia. Rather than a sign of dysfunction, hypothermia may represent an active host response in scenarios where the energy cost to maintain or increase body temperature exceeds its disease-fighting benefits. In these scenarios, hypothermia is employed as a disease-tolerance strategy[25]. Although *PA* grows at temperatures ranging from 4°C to over 42°C, it grows optimally at 37°C[36] and is thus routinely grown in the lab at 37°C. Moreover, prior studies suggest that *PA* has evolved

to respond to increases of temperature in its environment by reprogramming the expression of genes that support growth, colonization, and the expression of virulence factors, thereby gaining peak virulence at ~37°C [47, 48]. Nevertheless, two observations suggest that the mice do not actively employ hypothermia to limit the viability/virulence of the pathogen. First, as shown in Fig. 3A, the animals clearly exhibit heat- rather than cold-seeking behaviors and attempt to gain/maintain body heat by huddling, if kept at RT, or from increasing surface exposure to the cage bottom, if cages are placed on heating mats. Thus, while undergoing hypothermia may be critical to conserve energy reserves, the animals do employ mechanisms of maintaining elevated body temperatures (such as heat-seeking behavior) that come at little energetic cost. Second, that alleviating hypothermia from its very onset (Supplementary Fig. S10) improves bacterial clearance and survival of PDE4B-KO mice compared to WT littermates (Fig. 1M), by itself, suggests that the benefits of elevated body temperature on the host immune response, by far outweigh any benefits the pathogen may derive from the higher temperatures.

4.3. *P. aeruginosa*-induced hypothermia in “mice and men”.

Similar to mice, critically ill patients also undergo hypothermia, or cycle through phases of hypo- and hyperthermia. Although hypothermia correlates with poor outcomes in septic patients, this may not reflect causality, but rather the fact that hypothermic patients are sicker than others[25]. We show here that alleviating the *PA*-induced and cytokine-mediated hypothermia is a critical mechanism whereby PDE4B ablation improves bacterial clearance and, thus, ameliorates injury and mortality in a model of acute *PA*-lung infection in mice (Figs. 1/2). This is further illustrated by the fact that external warming produces a pattern of effects reminiscent of those produced by PDE4B ablation (Fig. 3), and that bacterial clearance in PDE4B-KO mice is not different from that of WT controls (Fig. 3K and Supplementary Fig. S14), when body temperatures are equalized by placing both groups on heating mats (Fig. 3J). As the magnitude of temperature loss in humans (1–3°C) is generally smaller than that in mice, and because hypothermia in the clinical setting can be effectively alleviated by external interventions (e.g. active rewarming), preventing hypothermia may not represent a critical therapeutic benefit that would be derived from pharmacologic PDE4B inactivation in humans. Nevertheless, the observation that development of the *PA*-induced cytostorm is dependent upon the induction of PDE4B/PDE4B2 expression in response to signaling of PAMPs (e.g. LPS/TLR4) and the primary response cytokines TNF-α and IL-1β in both mice and in cell culture, and that genetic deletion and/or the siRNA-mediated knockdown of PDE4B can alleviate the cytostorm by reducing the production of critical primary- and secondary-response cytokines (e.g. IL-6) suggests that targeting of PDE4B may realize therapeutic benefits by alleviating a cytokine storm also in the clinical setting, and may do so without impairing the clearance of the pathogen. The relevance of this insight may extend to the current SARS-CoV-2 pandemic, given that a cytokine signature comprising TNF-α, IL-1β, and IL-6 has been causally linked to poor health outcomes[49], and that IL-6 receptor blockers exert therapeutic benefits in critically ill COVID-19 patients[50].

Supplementary Material

Refer to Web version on PubMed Central for supplementary material.

Acknowledgments:

We are grateful to the entire staff of the Department of Comparative Medicine at the University of South Alabama for providing excellent care of the animals and their advice on experimental design. We are indebted to Drs. Sabrina Ramelli and William T. Gerthoffer for advice on developing intranasal infection, broncho-alveolar lavage and flow cytometry protocols, to Drs. Jonathan Scammell and Brian Fouty for advice on statistics and study design, to Drs. Jon Audia, Nicole Housley, and Sarah Voth for advice on bacterial infections, and to Trinh Le, Dylan Southers, and Edward Fiedler for technical assistance with experiments.

This work was supported by grants from the Cystic Fibrosis Foundation (SALEH18HO, SALEH19HO, RICHTE16GO), the National Institutes of Health (HL076125, HL141473, HL066299), and the USA College of Medicine Dean's Predoctoral Fellowship Program (LA, AB).

Abbreviations:

BAL
Broncho alveolar lavage

BALF
Broncho alveolar lavage fluid

DAMP
Damage-associated molecular pattern

EBD
Evans Blue Dye

IL
interleukin

IP
Immunoprecipitation

LPS
Lipopolysaccharide

MEF
Mouse embryonic fibroblast

MPO
Myeloperoxidase

PA
Pseudomonas aeruginosa

PAMP
Pathogen-associated molecular pattern

PBS
Phosphate-buffered saline

PDE

cyclic nucleotide phosphodiesterase

RT
room temperature

TLR
Toll-like receptor

TNF
Tumor necrosis factor

References

1. Micek ST, Kollef MH, Torres A, et al.Pseudomonas aeruginosa nosocomial pneumonia: impact of pneumonia classification. Infect Control Hosp Epidemiol. 102015;36(10):1190–7. doi:10.1017/ice.2015.167 [PubMed: 26190444]
2. Sawa TThe molecular mechanism of acute lung injury caused by Pseudomonas aeruginosa: from bacterial pathogenesis to host response. J Intensive Care. 2014;2(1):10. doi:10.1186/2052-0492-2-10 [PubMed: 25520826]
3. Fitzgerald M, McAuley DF, Matthay M. Is there a need for emerging drugs for the acute respiratory distress syndrome?Expert Opin Emerg Drugs. 92014;19(3):323–8. doi:10.1517/14728214.2014.953052 [PubMed: 25152048]
4. Li H, Zuo J, Tang W. Phosphodiesterase-4 Inhibitors for the Treatment of Inflammatory Diseases. Front Pharmacol. 2018;9:1048. doi:10.3389/fphar.2018.01048 [PubMed: 30386231]
5. Houslay MD, Schafer P, Zhang KY. Keynote review: phosphodiesterase-4 as a therapeutic target. Drug Discov Today. 11152005;10(22):1503–19. doi:S1359–6446(05)03622–6 [pii] 10.1016/S1359-6446(05)03622-6 [PubMed: 16257373]
6. Zhang KY, Ibrahim PN, Gillette S, Bollag G. Phosphodiesterase-4 as a potential drug target. Expert Opin Ther Targets. 122005;9(6):1283–305. doi:10.1517/14728222.9.6.1283 [PubMed: 16300476]
7. Baillie GS, Tejeda GS, Kelly MP. Therapeutic targeting of 3',5'-cyclic nucleotide phosphodiesterases: inhibition and beyond. Nat Rev Drug Discov. 102019;18(10):770–796. doi:10.1038/s41573-019-0033-4 [PubMed: 31388135]
8. Conti M, Richter W, Mehats C, Livera G, Park JY, Jin C. Cyclic AMP-specific PDE4 phosphodiesterases as critical components of cyclic AMP signaling. J Biol Chem. 22003;278(8):5493–6. doi:10.1074/jbc.R200029200 [PubMed: 12493749]
9. Richter W, Menniti FS, Zhang HT, Conti M. PDE4 as a target for cognition enhancement. Expert Opin Ther Targets. 72013;doi:10.1517/14728222.2013.818656
10. Jin SL, Conti M. Induction of the cyclic nucleotide phosphodiesterase PDE4B is essential for LPS-activated TNF-alpha responses. Proc Natl Acad Sci U S A. 52002;99(11):7628–33. doi:10.1073/pnas.122041599 [PubMed: 12032334]
11. Jin SL, Lan L, Zoudilova M, Conti M. Specific role of phosphodiesterase 4B in lipopolysaccharide-induced signaling in mouse macrophages. J Immunol. 812005;175(3):1523–31. doi:175/3/1523 [pii] [PubMed: 16034090]
12. Jin SL, Goya S, Nakae S, et al.Phosphodiesterase 4B is essential for T(H)2-cell function and development of airway hyperresponsiveness in allergic asthma. J Allergy Clin Immunol. 122010;126(6):1252–9 e12. doi:S0091–6749(10)01200–5 [pii] 10.1016/j.jaci.2010.08.014 [PubMed: 21047676]
13. Ma H, Shi J, Wang C, et al.Blockade of PDE4B limits lung vascular permeability and lung inflammation in LPS-induced acute lung injury. Biochem Biophys Res Commun. 82014;450(4):1560–7. doi:10.1016/j.bbrc.2014.07.024 [PubMed: 25019986]
14. Mika D, Richter W, Westenbroek RE, Catterall WA, Conti M. PDE4B mediates local feedback regulation of β_1-adrenergic cAMP signaling in a sarcolemmal compartment of cardiac myocytes. J Cell Sci. 32014;127(Pt 5):1033–42. doi:10.1242/jcs.140251 [PubMed: 24413164]

15. Blackman BE, Horner K, Heidmann J, et al.PDE4D and PDE4B function in distinct subcellular compartments in mouse embryonic fibroblasts. J Biol Chem. 42011;286(14):12590–601. doi:10.1074/jbc.M110.203604 [PubMed: 21288894]
16. Huston E, Lynch MJ, Mohamed A, et al.EPAC and PKA allow cAMP dual control over DNA-PK nuclear translocation. Proc Natl Acad Sci U S A. 922008;105(35):12791–6. doi:0805167105 [pii] 10.1073/pnas.0805167105 [PubMed: 18728186]
17. Kasetty G, Papareddy P, Bhongir RK, Egesten A. Roflumilast Increases Bacterial Load and Dissemination in a Model of Pseudomononas Aeruginosa Airway Infection. J Pharmacol Exp Ther. 42016;357(1):66–72. doi:10.1124/jpet.115.229641 [PubMed: 26865680]
18. Misharin AV, Morales-Nebreda L, Mutlu GM, Budinger GRS, Perlman H. Flow Cytometric Analysis of Macrophages and Dendritic Cell Subsets in the Mouse Lung. Am. J. Respir. Cell Mol. Biol. 2013102013;doi:10.1165/rcmb.2013-0086MA
19. Yu Y-RA, O'Koren EG, Hotten DF, et al.A Protocol for the Comprehensive Flow Cytometric Analysis of Immune Cells in Normal and Inflamed Murine Non-Lymphoid Tissues. Plos One. 20162016;doi:10.1371/journal.pone.0150606
20. GORRILL RH. Spinning disease of mice. The Journal of pathology and bacteriology. 195641956;71(2)doi:10.1002/path.1700710209
21. Xie M, Blackman B, Scheitrum C, et al.The upstream conserved regions (UCRs) mediate homo- and hetero-oligomerization of type 4 cyclic nucleotide phosphodiesterases (PDE4s). Biochem J. 52014;459(3):539–50. doi:10.1042/BJ20131681 [PubMed: 24555506]
22. Engel J, Balachandran P. Role of Pseudomonas aeruginosa type III effectors in disease. Curr Opin Microbiol. 22009;12(1):61–6. doi:10.1016/j.mib.2008.12.007 [PubMed: 19168385]
23. Hauser AR. The type III secretion system of Pseudomonas aeruginosa: infection by injection. Nat Rev Microbiol. 92009;7(9):654–65. doi:10.1038/nrmicro2199 [PubMed: 19680249]
24. Soares A, Alexandre K, Etienne M. Tolerance and Persistence of Pseudomonas aeruginosa in Biofilms Exposed to Antibiotics: Molecular Mechanisms, Antibiotic Strategies and Therapeutic Perspectives. Frontiers in microbiology. 8/27/20202020;11doi:10.3389/fmicb.2020.02057
25. Garami A, Steiner AA, Romanovsky AA. Fever and hypothermia in systemic inflammation. Handb Clin Neurol. 2018;157:565–597. doi:10.1016/B978-0-444-64074-1.00034-3 [PubMed: 30459026]
26. Rudaya AY, Steiner AA, Robbins JR, Dragic AS, Romanovsky AA. Thermoregulatory responses to lipopolysaccharide in the mouse: dependence on the dose and ambient temperature. Am J Physiol Regul Integr Comp Physiol. 112005;289(5):R1244–52. doi:10.1152/ajpregu.00370.2005 [PubMed: 16081879]
27. Romanovsky AA, Almeida MC, Aronoff DM, et al.Fever and hypothermia in systemic inflammation: recent discoveries and revisions. Front Biosci. 92005;10:2193–216. doi:10.2741/1690 [PubMed: 15970487]
28. Leon LR. Hypothermia in systemic inflammation: role of cytokines. Frontiers in bioscience : a journal and virtual library. 5/01/20042004;9doi:10.2741/1381
29. Ariga M, Neitzert B, Nakae S, et al.Nonredundant function of phosphodiesterases 4D and 4B in neutrophil recruitment to the site of inflammation. J Immunol. 12152004;173(12):7531–8. doi:173/12/7531 [pii] [PubMed: 15585880]
30. Gordon CJ. The mouse thermoregulatory system: Its impact on translating biomedical data to humans. Physiol Behav. 1012017;179:55–66. doi:10.1016/j.physbeh.2017.05.026 [PubMed: 28533176]
31. Skelly DT, Hennessy E, Dansereau MA, Cunningham C. A systematic analysis of the peripheral and CNS effects of systemic LPS, IL-1β, TNF-α and IL-6 challenges in C57BL/6 mice. PloS one. 7/01/20132013;8(7)doi:10.1371/journal.pone.0069123
32. Van Linthout S, Miteva K, Tschöpe C. Crosstalk between fibroblasts and inflammatory cells. Cardiovascular research. 5/01/20142014;102(2)doi:10.1093/cvr/cvu062
33. Tavares LP, Negreiros-Lima GL, Lima KM, et al.Blame the signaling: Role of cAMP for the resolution of inflammation. Pharmacological research. 202092020;159doi:10.1016/j.phrs.2020.105030

34. Lima KM, Vago JP, Caux TR, et al.The resolution of acute inflammation induced by cyclic AMP is dependent on annexin A1. The Journal of biological chemistry. 8/18/20172017;292(33)doi:10.1074/jbc.M117.800391
35. Park T, Chen H, Kevala K, Lee JW, Kim HY. N-Docosahexaenoylethanolamine ameliorates LPS-induced neuroinflammation via cAMP/PKA-dependent signaling. Journal of neuroinflammation. 11/04/20162016;13(1)doi:10.1186/s12974-016-0751-z
36. Tsuji A, Kaneko Y, Takahashi K, Ogawa M, Goto S. The effects of temperature and pH on the growth of eight enteric and nine glucose non-fermenting species of gram-negative rods. Microbiology and immunology. 19821982;26(1)doi:10.1111/j.1348-0421.1982.tb00149.x
37. Gazmuri RJ, Gopalakrishnan P. Hypothermia: cooling down inflammation. Crit Care Med. 122003;31(12):2811–2. doi:10.1097/01.ccm.0000099344.57796.f3 [PubMed: 14668624]
38. Geurts M, Macleod MR, Kollmar R, Kremer PH, van der Worp HB. Therapeutic hypothermia and the risk of infection: a systematic review and meta-analysis. Crit Care Med. 22014;42(2):231–42. doi:10.1097/CCM.0b013e3182a276e8 [PubMed: 23989182]
39. Soares AC, Souza DG, Pinho V, et al.Impaired host defense to Klebsiella pneumoniae infection in mice treated with the PDE4 inhibitor rolipram. British journal of pharmacology. 2003112003;140(5)doi:10.1038/sj.bjp.0705517
40. Tavares LP, Garcia CC, Vago JP, et al.Inhibition of Phosphodiesterase-4 during Pneumococcal Pneumonia Reduces Inflammation and Lung Injury in Mice. American journal of respiratory cell and molecular biology. 201672016;55(1)doi:10.1165/rcmb.2015-0083OC
41. McDonough W, Rich J, Aragon IV, et al.Inhibition of type 4 cAMP-phosphodiesterases (PDE4s) in mice induces hypothermia via effects on behavioral and central autonomous thermoregulation. Biochemical pharmacology. 7/20/20202020;180doi:10.1016/j.bcp.2020.114158
42. McDonough W, Aragon IV, Rich J, et al.PAN-selective inhibition of cAMP-phosphodiesterase 4 (PDE4) induces gastroparesis in mice. FASEB journal : official publication of the Federation of American Societies for Experimental Biology. 8/01/20202020;doi:10.1096/fj.202001016RR
43. Aragon IV, Boyd A, Abou Saleh L, et al.Inhibition of cAMP-phosphodiesterase 4 (PDE4) potentiates the anesthetic effects of Isoflurane in mice. Biochemical pharmacology. 2/17/20212021;doi:10.1016/j.bcp.2021.114477
44. Suzuki O, Mizukami K, Etori M, et al.Evaluation of the therapeutic index of a novel phosphodiesterase 4B-selective inhibitor over phosphodiesterase 4D in mice. J Pharmacol Sci. 2013;123(3):219–26. [PubMed: 24152964]
45. Robichaud A, Stamatiou PB, Jin SL, et al.Deletion of phosphodiesterase 4D in mice shortens alpha(2)-adrenoceptor-mediated anesthesia, a behavioral correlate of emesis. J Clin Invest. 102002;110(7):1045–52. doi:10.1172/jci15506 [PubMed: 12370283]
46. Romanovsky AA. The thermoregulation system and how it works. Handb Clin Neurol. 2018;156:3–43. doi:10.1016/B978-0-444-63912-7.00001-1 [PubMed: 30454596]
47. Grosso-Becerra MV, Croda-García G, Merino E, Servín-González L, Mojica-Espinosa R, Soberón-Chávez G. Regulation of Pseudomonas aeruginosa virulence factors by two novel RNA thermometers. Proceedings of the National Academy of Sciences of the United States of America. 10/28/20142014;111(43)doi:10.1073/pnas.1402536111
48. Barbier M, Damron FH, Bielecki P, et al.From the environment to the host: re-wiring of the transcriptome of Pseudomonas aeruginosa from 22°C to 37°C. PloS one. 2/24/20142014;9(2)doi:10.1371/journal.pone.0089941
49. Del Valle DM, Kim-Schulze S, Huang HH, et al.An inflammatory cytokine signature predicts COVID-19 severity and survival. Nature medicine. 2020102020;26(10)doi:10.1038/s41591-020-1051-9
50. Gordon AC, Mouncey PR, Al-Beidh F, et al.Interleukin-6 Receptor Antagonists in Critically Ill Patients with Covid-19. The New England journal of medicine. 2/25/20212021;doi:10.1056/NEJMoa2100433

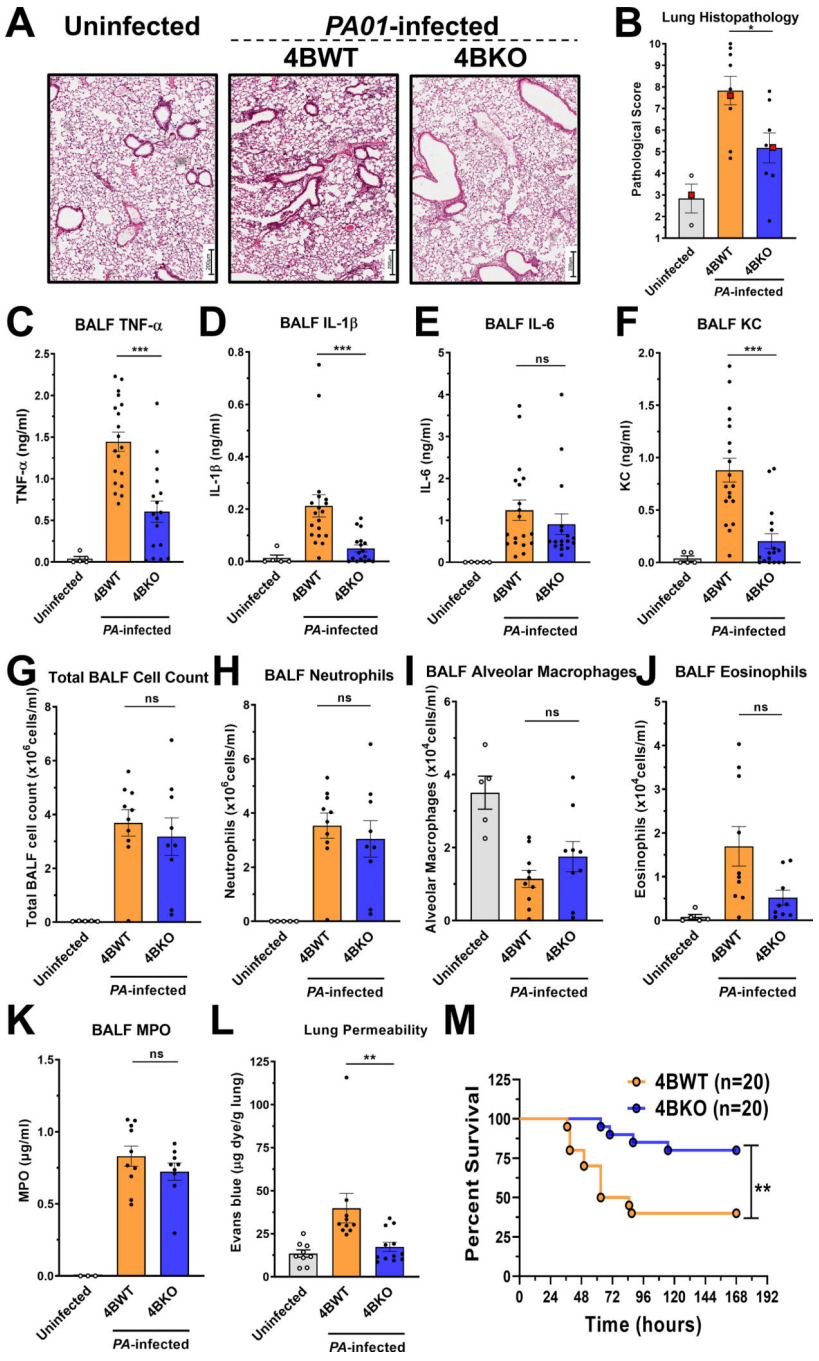

Fig. 1. PDE4B ablation protects from *P. aeruginosa*-induced lung injury.

(**A-K**) Lung injury in PDE4B-KO mice (4BKO) and wildtype (4BWT) littermate controls was assessed at 16 h after intranasal infection with strain *PA01* (*PA*-infected) or sterile PBS (Uninfected). (**A/B**) Infection with *PA01* causes lung tissue inflammation characterized by neutrophilia. 4BKO mice are protected from *PA01*-induced lung injury as determined by lung histopathologic scoring (the red squares in (**B**) indicate the lung sections shown in (**A**)), and reduced levels of pro-inflammatory cytokines in BALF (**C-F**). (**G-K**) At 16 h post infection, the number of total leukocytes (**G**), neutrophils (**H**), alveolar macrophages

(**I**), and eosinophils (**J**), as well as the levels of myeloperoxidase (MPO) in BALF (**K**) are not changed by PDE4B ablation. (**L**) Ablation of PDE4B protects from pulmonary vascular leakage as reflected by the level of extravasation of Evans Blue Dye measured at 16 h post infection. (**M**) Ablation of PDE4B improves the 7-day survival rate of mice. All data represent mean ± SEM. For 7-day survival, statistical significance was determined using the Mantel-Cox log-rank test; for all other graphs, statistical significance was determined using Mann-Whitney test and is indicated as ns (not significant), * ($p<0.05$), ** ($p<0.01$), or *** ($p<0.001$).

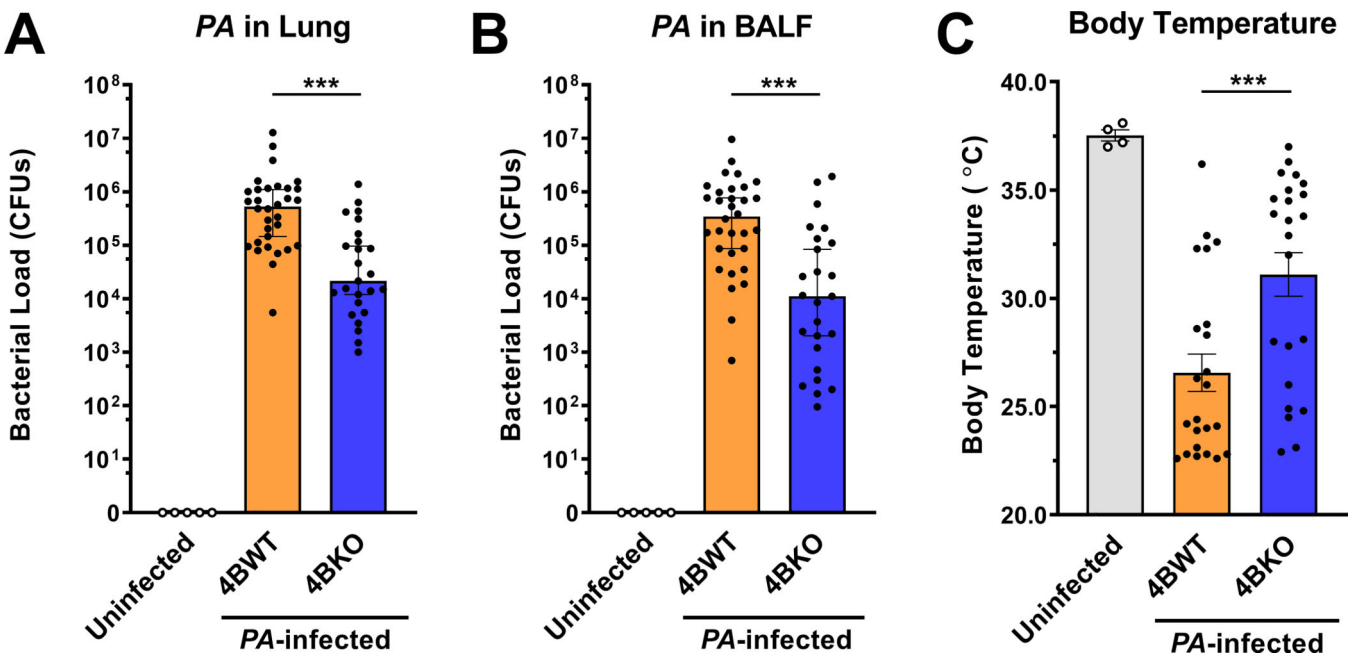

Fig. 2. Improved bacterial clearance and allayed hypothermia in mice deficient in PDE4B.

16 h after intranasal infection with *PA01* (*PA*-infected) or PBS (Uninfected), the body temperature of mice was measured, and animals were then subjected to broncho-alveolar lavage (BAL) followed by extraction of the lungs. (**A/B**) Bacterial load was determined by plating serial dilutions of (**A**) right lung tissue homogenates or (**B**) BALF on agar plates. Data represent the median with 95% CI. (**C**) Core body temperature at 16 h post infection measured using a rectal thermometer. Data represent the mean ± SEM. Statistical significance was determined using Mann-Whitney test and is indicated as *** ($p<0.001$)

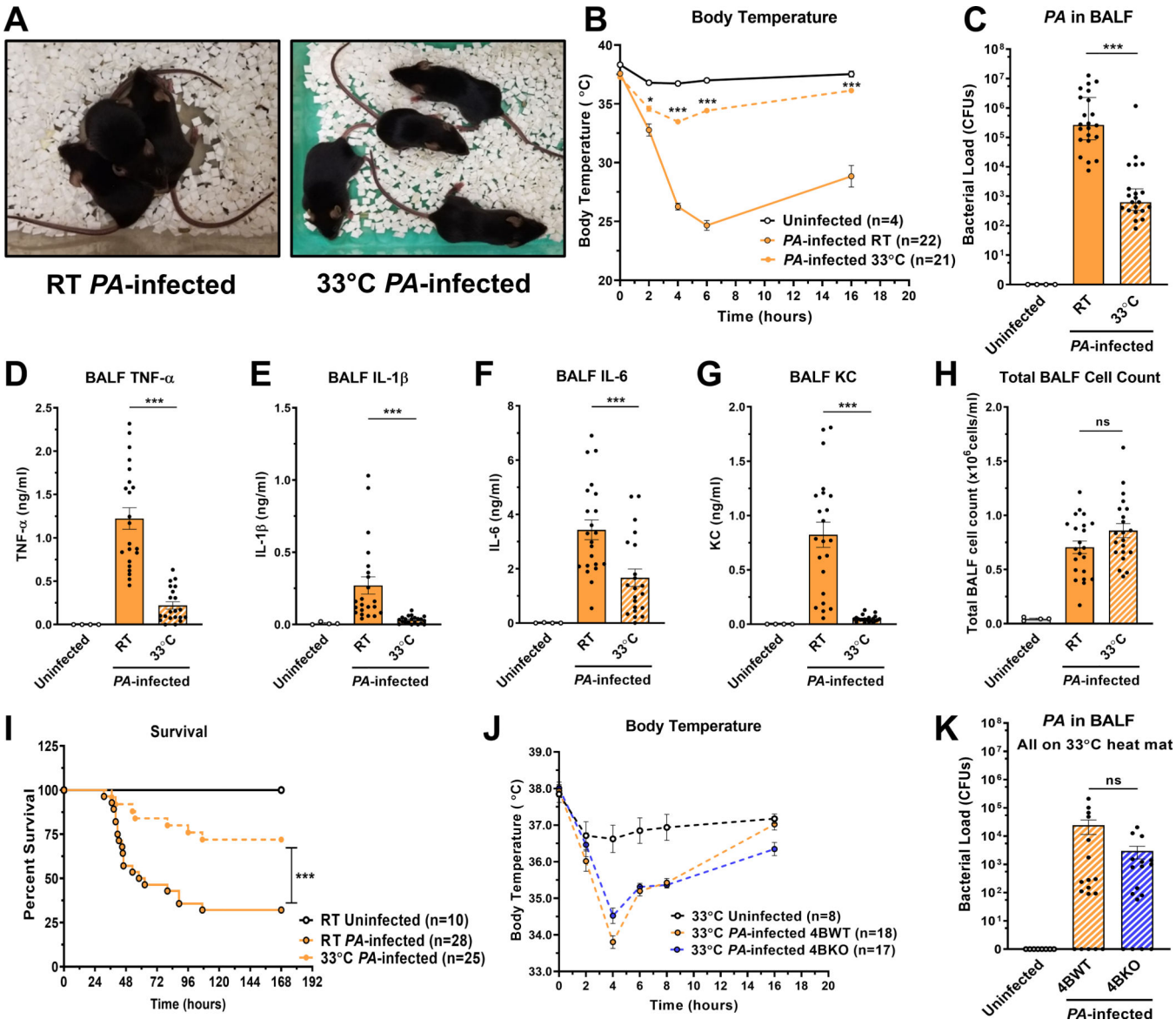

Fig. 3. Alleviating hypothermia with external heat protects from *PA*-induced lung injury and improves bacterial clearance.

(**A**) After intranasal infection with *PA01*, WT mice were either kept at room temperature (RT), left image, or cages were placed on an external heating mat set to 33°C, right image (the mat is visible in green beneath the cage), for 16 h post-infection. At this time point, the mice exhibit clear heat-seeking behaviors as indicated by the representative images. Mice kept at RT characteristically huddle-up to each other. Conversely, mice on the 33°C heat mat characteristically spread out flat to maximize heat absorbance through the cage bottom. (**B-H**) Placing cages on a 33°C heating mat (striated lines and columns) alleviates *PA*-induced hypothermia compared to mice kept at RT (solid lines and columns) (**B**) and reduces the bacterial load in BALF (**C**) as well as the levels of pro-inflammatory cytokines (**D-G**) measured at 16 h post-infection. Conversely, the total number of leukocytes in BALF is unchanged (**H**). (**I**) Placing cages on a 33°C heat mat upon infection with *PA01* improves the

survival of WT mice. (**J**/**K**) Placing PDE4B-knockout (4BKO) mice and wildtype (4BWT) littermate controls on a 33°C heat mat ablates differences in their body temperature upon *PA01* infection (**J**), as well as differences in bacterial load in BALF (**K**) that were observed in mice kept at RT (see Fig. 1). Data represent the mean ± SEM (**B**, **D**-**J**), or the median with 95% CI (**C**/**K**). Statistical significance was determined using two-way ANOVA with Tukey's multiple comparisons test (**B**/**J**), Mann-Whitney test (**C**-**H**, **K**), or Mantel-Cox log-rank test (**I**), and is indicated as ns (not significant), * ($p<0.05$), ** ($p<0.01$), *** ($p<0.001$).

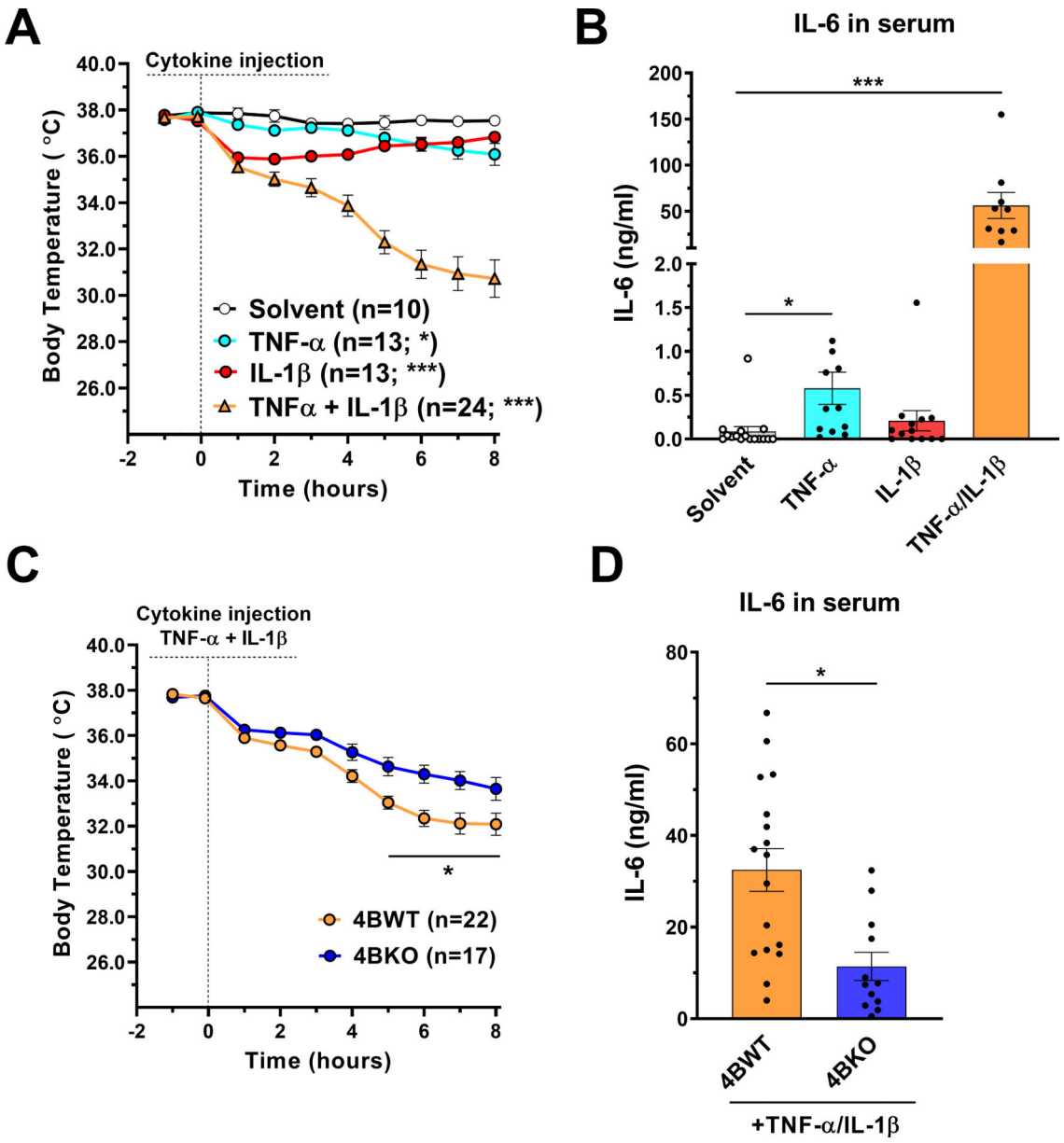

Fig. 4. PDE4B ablation protects from hypothermia induced by injection of the acute-response cytokines TNF-α and IL-1β.

Mice were injected intraperitoneally with PBS (Solvent), TNF-α (2.5 μg/20 g mouse) and/or IL-1β (1 μg/20 g mouse) and core body temperature was subsequently measured once every hour. In some experiments, mice were euthanized eight hours after cytokine injection, subjected to cardiac blood draws, and IL-6 levels were measured in the resulting serum samples. (**A**) TNF-α and IL-1β act synergistically to induce substantial hypothermia in mice. (**B**) The levels of hypothermia induced by TNF-α and IL-1β are paralleled by the induction of systemic IL-6 levels. (**C/D**) Mice deficient in PDE4B are partially protected from TNF-α/IL-1β-induced hypothermia (**C**) and associated IL-6 production (**D**). Data shown represent the mean ± SEM. Statistical significance was determined using Mann-

Whitney test (bar graphs) or two-way ANOVA with Tukey's multiple comparisons test (time courses) and is indicated as * ($p<0.05$) or *** ($p<0.001$).

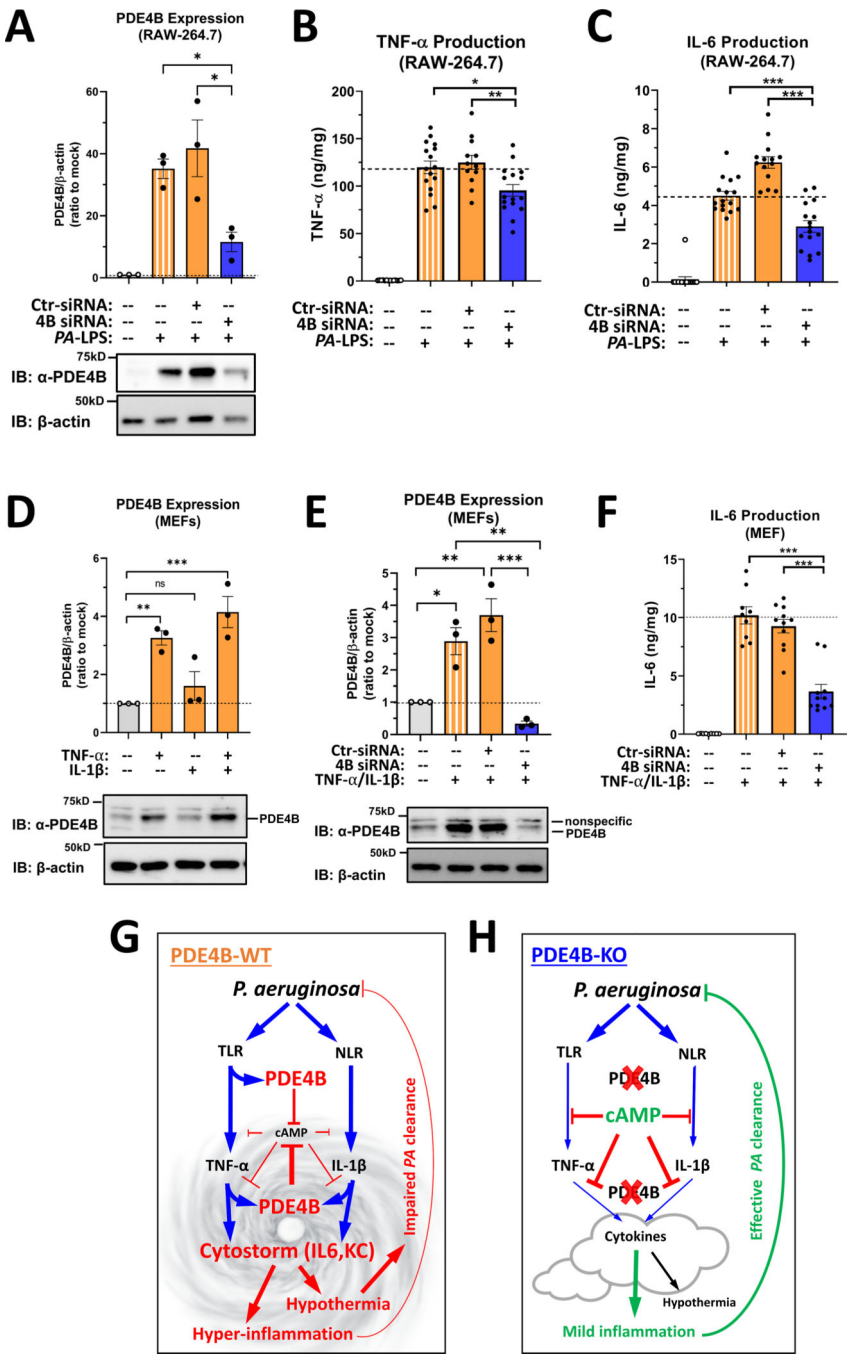

Fig. 5. Inactivation of PDE4B acts downstream of PAMP- and cytokine-receptors to alleviate production of pro-inflammatory cytokines.

(**A-F**) RAW-264.7 mouse macrophages and mouse embryonic fibroblasts (MEFs) grown in cell culture were treated for 6 h with *PA*-LPS (10 μg/ml), TNF-α (0.01 μg/ml) and/or IL-1β (0.1 μg/ml) before cells and cell supernatants were harvested to probe PDE4B expression by Western blotting or cytokine production by ELISA, respectively. In some experiments, cells were transfected with siRNA targeting PDE4B (4B siRNA) or negative control siRNA (Ctr-siRNA) for 42 h prior to cell treatment. (**A-C**) Treatment of RAW-264.7 macrophages

with *PA*-LPS induces expression of PDE4B (**A**) and the production of TNF-α (**B**) and IL-6 (**C**), all of which are curbed by the siRNA-mediated knockdown of PDE4B. (**D-F**) MEFs respond to treatment with TNF-α and/or IL-1β with a substantial induction of PDE4B protein expression and production of IL-6, both of which are reversed by siRNA-mediated PDE4B knockdown. All graphs represent mean ± SEM. Statistical analysis was determined using one-way ANOVA with Tukey's multiple comparison test and is indicated as ns (not significant; $p>0.05$), * ($p<0.05$), ** ($p<0.01$), or *** ($p<0.001$). (**G/H**) **Schemes illustrating the effect of PDE4B ablation on *P. aeruginosa*-induced acute lung injury in mice.** Elevated cAMP levels exert a negative constraint on the production of primary-response cytokines induced by activation of PAMP-receptors (e.g. Toll-like and NOD-like receptors) as well as on the induction of secondary-response cytokines that are induced by activation of cytokine-receptors (e.g. TNF-α and IL-1β). In WT cells and animals (**G**), *PA*-induced signaling of PAMP- and cytokine receptors also induced expression of PDE4B, which in turn lowers cellular cAMP levels, thus promoting a hyperinflammatory response dubbed "cytostorm". Pro-inflammatory cytokines do not only promote recruitment and activation of immune cells, but also act as cryogens, leading to significant hypothermia, which in turn hampers clearance of the bacteria. Conversely, if induction of PDE4B expression is prevented *via* gene knockout or knockdown, the negative constraint of cAMP signaling is retained, resulting in the alleviated cytokine levels that are sufficient to muster an effective immune cell recruitment and bacterial clearance, in part because *PA*-induced hypothermia is alleviated (**H**).